Supporting Information

A 3D Lead Chloride Hybrid Exhibits Self-Trapped Emission and Exceptional Stability

Mohamed Saber Lassoued[a], [b], [c], Qian-Cheng Luo[b], and Yan-Zhen Zheng[a], [b], [c]*

[a] School of Chemistry, Xi'an Jiaotong University, 99 Yanxiang Road, Xi'an, Shaanxi 710054, P R. China.

[b] Frontier Institute of Science and technology, Xi'an Jiaotong University, 99 Yanxiang Road, Xi'an, Shaanxi 710054, P R. China.

[c] State Key Laboratory of Electrical Insulation and Power Equipment, Xi'an Jiaotong University, 28 Xianning West Road, Shaanxi 710049, P. R. China.

Corresponding author (ZYZ): zheng.yanzhen@xjtu.edu.cn

Table of content

1. General remarks

Single crystal X-ray diffraction data of $(H_2MPP)_2Pb_5Cl_{14}$ was collected on a Bruker SMART APEX II CCD diffractometer with graphite monochromated Mo-k radiation (λ= 0.71073 Å) by using the θ-ω scan technique at room temperature. PXRD intensities were measured at ambient temperature (298 K) on a Rigaku D/max-IIIA diffractometer (Cu-kλ, λ=1.54056 Å). The crystalline powder samples were prepared by grinding the single-crystals and collected in the 2θ range of [5°–50°] with a step size of 5°/min at room temperature. Scanning electron microscopy (SEM) was performed using KYKY-EM3200, 25 KV instrument. Solid-state UV-Vis diffusion reflectance spectra of pressed powder and films samples were measured on a SHIMADZU UV-3600 UV-Vis-NIR spectrophotometer using $BaSO_4$ powder as the reflectance reference. Steady-state emission spectra were collected on powder samples using an Edinburgh FLS985 fluorimeter upon 290 nm excitation. Decay lifetimes and photoluminescence quantum yield (PLQY) were obtained by Edinburgh Instruments of FLS 985. All density-functional theory (DFT) calculations were carried out within CASTEP software.

2. Characterization methods and Simulation details

2.1. Characterization methods

X-ray Crystallographic Study

Single-crystal X-ray diffraction data collections for $(H_2MPP)_2Pb_5Cl_{14}$ was conducted on a Bruker SMART APEX II CCD diffractometer (Mo, λ = 0.71073 Å) by using the θ-ω scan technique at 298 K. The structures were solved by direct methods and refined with a full-matrix least-squares technique within the SHELXTL program package. [S1] All non-hydrogen atoms were refined anisotropically. Powder X-ray difraction intensities were measured at ambient temperature (298 K) on a Rigaku D/max-IIIA diffractometer (Cu-kλ, λ=1.54056 Å). The crystallographic details are provided in Tables S1-S3. CCDC number of $(H_2MPP)_2Pb_5Cl_{14}$ is 2277762. The crystallographic data for above compounds can be found in the Supporting Information or can be obtained free of charge from the

Inorganic Crystal Structure Database via http://www.ccdc.cam.ac.uk/data_request/cif.

The crystalline powder samples were prepared by grinding the single-crystals and collected in the 2θ range of [5°–50°] with a step size of 5°/min at room temperature.

Morphology and elemental analysis: Scanning electron microscopy (SEM) was performed using KYKY-EM3200, 25 KV instrument attached with an Oxford X-MaxN energy dispersive X-ray spectroscope (EDS).

Optical measurement: Solid-state UV-Vis diffusion reflectance spectra of pressed powder and films samples were measured on a SHIMADZU UV-3600 UV-Vis-NIR spectrophotometer using $BaSO_4$ powder as the reflectance reference.

Photoluminiscence: Photoluminiscence excitation (PLE) and emission (PL), photoluminiscence quantum yield (PLQY) and the decay lif time were collected on powder samples or crystal samples using an Edinburgh FLS985 fluorimeter upon 365 nm excitation. Low temperature-dependent PL spectra were also obtained by Edinburgh FLS985 with the excitation wavelength at 290 nm.

Thermogravimetric Analysis: Thermogravimetric analyses (TGA) were carried out on a METTLER TOLEDO TGA/DSC3+ Extreme. A heating rate of 10 K min^{-1} under flowing N_2 was used from room temperature to 1050 K to investigate the thermal stabilities.

Electrical conductivities: 50 mg powder of $(H_2MPP)_2Pb_5Cl_{14}$ was used to press pellet (ϕ = 10 mm) with the thickness about 0.3 mm. Silver conductive paint (SPI supplies co.) was used to stick the wire and the pellet. To test the conductivity under different temperatures, we used an oven to control the temperature. We used a source meter (Keithley 2400) serving as a voltage source, and in series with a picoammeter (Keithley 6485) to detect the small currents. The electrical conductivity is calculated by the plots of current density versus electric field strength (J-E curves) based on the following Ohm's law: $\sigma = J / E$, $J = I / S$, $E = V / L$ where σ is the conductivity, J is the current density, E is the electric field strength, I is the current, V is the voltage, S is the cross-sectional area of the pressed pellets,

and L is the thickness of the pellets.

Stability measurements: Freshly prepared powder of $(H_2MPP)_2Pb_5Cl_{14}$ was deposited on clear plate glasses and thereafter they were placed inside sealed jar containing a saturated solution of $Mg(NO_3)_2.6H_2O$, stored either in the dark to minimize light exposure and the relative humidity was maintained at ~55% humidity. [S2] Powder sample was not in direct contact with the solution and was analyzed with PXRD after 60 days.

2.2 Simulation details and Computational methods. All the calculations in this work were carried out using density functional theory (DFT) as implemented in the BIOVIA Materials Studio Simulation Package. [S3, S4] The generalized gradient approximation (GGA) Perdew–Burke–Ernzerhof (PBE) functional was used for electronic structure calculations. [S5, S6] The convergence threshold for the self-consistent field was 2×10^{-6} eV/atom. The pseudopotential form was OTFG ultrasoft mode and the energy cutoff was 489.8 eV. The DFT calculation of $(H_2MPP)_2Pb_5Cl_{14}$ band structure were executed with or without. When excluding the spin orbit coupling (SOC), the kinetic energy cutoff we used was 260 eV with ultrasoft pseudopotentials. For the case of including the SOC, we applied norm conserving pseudopotentials and the kinetic energy cutoff was 600 eV.

3. Supporting Tables and Figures

Table S1. Crystal data and structure refinement for $(H_2MPP)_2Pb_5Cl_{14}$

Compound	$(H_2MPP)_2Pb_5Cl_{14}$
Empirical formula	$C_{12}\ H_{32}\ Cl_{14}\ N_4\ Pb_5$
Formula weight	1764.72
Crystal dimensions (mm)	0.34*0.27*0.14
Crystal system	Orthorhombic
Space group	I m a 2
a/Å	33.357(7)
b/Å	11.422(2)
c/Å	18.500(4)
α/°	90
β/°	90
γ/°	90
Volume/Å^3	7049(2)
Z	8
ρ calcg/cm^3	3.326
μ /mm^{-1}	24.881
F(000)	6240.0
Index ranges	-45<=h<=45, -15<=k<=15, -25<=l<=25
Data Completeness	100%
Data/restraints/parameters	8704/1/335
Goodness-of-fit on F2	1.06
Weight	$w = 1/[\sigma^2(Fo^2) + (0.0252P)^2 + 218.9547P]$ where $P = (Fo^2 + 2Fc^2)/3$
$R=\sum\|\|Fo-Fc\|\|/\sum\|Fo\|, wR_2$	$R_1 = 0.04$, $wR_2 = 0.091$

$R1 = \Sigma||Fo| - |Fc||/\Sigma|Fo|$, $wR_2 = [\Sigma w(Fo^2 - Fc^2)^2 / \Sigma w(Fo^2)^2]^{1/2}$

Table S2. Summary of selected bond lengths (Å) and bond angles (°) of $(H_2MPP)_2Pb_5Cl_{14}$

Bond	Lengths/Å	Bond pair	Angles / °	Bond pair	Angles / °
Pb2 Cl10	2.832(4)	Cl10 Pb2 Cl7	144.27(12)	Cl9 Pb3 Cl8	76.89(10)
Pb2 Cl7	3.004(4)	Cl10 Pb2 Cl8	77.64(10)	Cl8 Pb3 Cl8	71.85(14)
Pb2 Cl8	3.036(3)	Cl10 Pb2 Cl8	77.64(10)	Cl12 Pb7 Cl12	71.07(14
Pb2 Cl8	3.036(3)	Cl10 Pb2 Cl5	84.92(8)	Cl11 Pb7 Cl12	72.94(10
Pb2 Cl5	2.873(3)	Cl10 Pb2 Cl5	84.92(8)	Cl11 Pb7 Cl12	80.03(10
Pb2 Cl5	2.873(3)	Cl7 Pb2 Cl8	73.31(10)	Cl11 Pb7 Cl12	80.03(10
Pb1 Cl6	2.917(3)	Cl7 Pb2 Cl8	73.31(10)	Cl11 Pb7 Cl12	72.94(10
Pb1 Cl3	2.955(3)	Cl8 Pb2 Cl8	70.23(13)	Cl11 Pb7 Cl11	146.70(11)
Pb1 Cl2	2.910(3)	Cl5 Pb2 Cl7	108.36(7)	Cl12 Pb6 Cl12	70.94(13)
Pb1 Cl5	2.994(3)	Cl5 Pb2 Cl7	108.36(7)	Cl12 Pb6 Cl15	78.34(10)
Pb1 Cl4	2.922(4)	Cl5 Pb2 Cl8	77.84(9)	Cl12 Pb6 Cl11	78.66(9)
Pb1 Cl1	2.834(5)	Cl5 Pb2 Cl8	77.84(9)	Cl14 Pb6 Cl12	147.30(1
Pb4 Cl10	2.939(4	Cl5 Pb2 Cl8	146.13(9)	Cl14 Pb6 Cl12	77.09(10
Pb4 Cl9	2.836(5)	Cl5 Pb2 Cl8	146.13(9)	Cl14 Pb6 Cl15	132.45(1
Pb4 Cl3	2.947(3)	Cl5 Pb2 Cl5	129.61(13)	Cl14 Pb6 Cl11	97.58(10
Pb4 Cl3	2.947(3)	Cl6 Pb1 Cl3	145.33(9)	Cl15 Pb6 Cl12	148.93(1
Pb4 Cl8	2.983(3)	Cl6 Pb1 Cl5	71.74(10)	Cl13 Pb6 Cl12	76.83(9)
Pb4 Cl8	2.983(3)	Cl6 Pb1 Cl4	74.54(11)	Cl13 Pb6 Cl12	77.63(9)
Pb5 Cl17	2.832(3)	Cl3 Pb1 Cl5	138.05(10)	Cl13 Pb6 Cl14	88.75(8)
Pb5 Cl17	3.064(4)	Cl2 Pb1 Cl6	72.25(11)	Cl13 Pb6 Cl15	92.43(8)
Pb5 Cl14	3.044(4)	Cl2 Pb1 Cl3	74.40(11)	Cl13 Pb6 Cl11	144.83(1
Pb5 Cl15	2.923(4)	Cl2 Pb1 Cl5	142.81(9)	Cl11 Pb6 Cl12	71.06(9)
Pb5 Cl16	2.920(4)	Cl2 Pb1 Cl4	81.08(12)	Cl11 Pb6 Cl15	107.74(1
Pb5 Cl18	2.820(4)	Cl4 Pb1 Cl3	91.28(12)	Pb2 Cl10 Pb4	93.43(12)
Pb3 Cl7	2.867(4)	Cl4 Pb1 Cl5	80.74(12)	Pb1 Cl6 Pb1	89.15(11)
Pb3 Cl9	2.892(4)	Cl1 Pb1 Cl6	78.96(13)	Pb3 Cl7 Pb2	94.38(13)
Pb3 Cl8	2.976(4)	Cl1 Pb1 Cl3	107.29(11)	Pb4 Cl9 Pb3	92.94(13)
Pb3 Cl8	2.976(4)	Cl1 Pb1 Cl2	84.83(14)	Pb4 Cl3 Pb1	100.06(10)
Pb7 Cl12	3.003(4)	Cl1 Pb1 Cl5	97.15(11)	Pb1 Cl2 Pb1	89.43(13)
Pb7 Cl12	3.003(4)	Cl1 Pb1 Cl4	152.71(14)	Pb4 Cl8 Pb2	88.54(10)
Pb7 Cl11	2.889(3)	Cl10 Pb4 Cl3	95.66(8)	Pb3 Cl8 Pb2	91.53(10)
Pb7 Cl11	2.889(3)	Cl10 Pb4 Cl3	95.66(8)	Pb3 Cl8 Pb4	88.36(10)
Pb6 Cl12	3.032(4)	Cl10 Pb4 Cl8	76.88(10)	Pb2 Cl5 Pb1	99.99(10)
Pb6 Cl12	2.983(4)	Cl10 Pb4 Cl8	76.88(10)	Pb1 Cl4 Pb1	88.95(16)
Pb6 Cl14	2.838(3)	Cl9 Pb4 Cl10	148.41(13	Pb7 Cl12 Pb6	90.13(10)
Pb6 Cl15	3.015(3)	Cl9 Pb4 Cl3	97.11(8)	Pb6 Cl12 Pb7	91.07(10)
Pb6 Cl13	2.834(3)	Cl9 Pb4 Cl3	97.11(8)	Pb6 Cl12 Pb6	87.79(10)
Pb6 Cl11	2.996(4)	Cl9 Pb4 Cl8	77.62(10)	Pb5 Cl17 Pb5	89.85(10)
Cl6 Pb1	2.917(3)	Cl9 Pb4 Cl8	77.62(10)	Pb6 Cl14 Pb5	102.08(10

Cl3 Pb4	2.947(3)	Cl3 Pb4 Cl3	131.76(12)	Pb5 Cl15 Pb6	96.07(10)
Cl2 Pb1	2.910(3)	Cl3 Pb4 Cl8	78.28(9) 3	Pb6 Cl13 Pb6	94.78(14)
Cl4 Pb1	2.922(4)	Cl3 Pb4 Cl8	149.92(9)	Pb7 Cl11 Pb6	93.09(10)
Cl12 Pb6	3.032(4)	Cl3 Pb4 Cl8	149.92(9)	Pb5 Cl16 Pb5	91.07(16)
Cl17 Pb5	3.064(4)	Cl3 Pb4 Cl8	78.28(9)	C12 N3 C7	109.2(10)
Cl14 Pb5	3.044(4)	Cl8 Pb4 Cl8	71.66(14)	C11 N3 C7	112.3(10)
Cl13 Pb6	2.834(3)	Cl17 Pb5 Cl17	71.45(12)	C11 N3 C12	111.8(12)
Cl11 Pb6	2.996(4)	Cl17 Pb5 Cl14	140.11(10)	C4 N1 C3	110.0(9)
Cl16 Pb5	2.920(4)	Cl17 Pb5 Cl15	75.81(10)	C6 N1 C4	111.1(10)
N3 C7	1.529(17)	Cl17 Pb5 Cl16	78.94(10)	C6 N1 C3	111.8(10)
N3 C12	1.485(19)	Cl14 Pb5 Cl17	69.33(9)	C8 C7 N3	110.7(11)
N3 C11	1.481(17)	Cl15 Pb5 Cl17	146.13(9)	C5 C4 N1	111.8(10)
N1 C4	1.497(17)	Cl15 Pb5 Cl14	140.66(11)	C7 C8 C9	112.7(11)
N1 C6	1.488(17)	Cl16 Pb5 Cl17	75.30(10)	N4 C9 C8	108.3(11)
N1 C3	1.553(16)	Cl16 Pb5 Cl14	84.41(7)	N4 C9 C10	112.5(11)
N4 C9	1.473(17)	Cl16 Pb5 Cl15	90.30(8)	C10 C9 C8	109.6(10)
C7 C8	1.50(2)	Cl18 Pb5 Cl17	78.13(12)	C9 C10 C11	110.2(11)
C4 C5	1.491(18)	Cl18 Pb5 Cl17	84.69(13)	N2 C1 C2	110.9(10)
N2 C1	1.461(17)	Cl18 Pb5 Cl14	94.15(10)	N2 C1 C5	108.7(11)
C8 C9	1.536(18)	Cl18 Pb5 Cl15	107.51(10)	C2 C1 C5	108.4(10)
C9 C10	1.516(18)	Cl18 Pb5 Cl16	152.08(10)	C3 C2 C1	110.6(11)
C10 C11	1.529(19)	Cl7 Pb3 Cl9	146.56(13)	C4 C5 C1	111.4(11)
C1 C2	1.534(18)	Cl7 Pb3 Cl8	76.17(9)	N3 C11 C10	109.8(11)
C1 C5	1.538(18)	Cl7 Pb3 Cl8	76.17(9)	C2 C3 N1	106.3(10)
C2 C3	1.500(18)	Cl9 Pb3 Cl8	76.89(10)		

Table S3. Potential hydrogen bonding data of $(H_2MPP)_2Pb_5Cl_{14}$

D-H	d(D-H)	d(H..A)	<DHA	d(D..A)	A	
N3-H3	0.909	2.67	119.6	3.217	Cl5	[x, y-1, z]
N3-H3	0.909	2.721	152.84	3.554	Cl8	[x, y-1, z]
N1-H1	0.911	2.598	150.7	3.421	Cl12	[-x+1, -y+2, z]
N1-H1	0.911	2.692	118.92	3.232	Cl14	
N4-H4A	0.889	2.577	144.64	3.342	Cl11	[-x+1, y-1/2, z-1/2]
N4-H4A	0.889	2.922	112.33	3.362	Cl18	[-x+1, -y+2, z]
N4-H4A	0.889	2.936	116.86	3.43	Cl17	[x, y-1, z]
N4-H4B	0.889	2.411	153.41	3.231	Cl14	[x, y-1, z]
N4-H4C	0.891	2.32	167.99	3.197	Cl3	
N2-H2A	0.891	2.652	129.53	3.291	Cl5	
N2-H2A	0.891	2.67	137.68	3.382	Cl10	
N2-H2B	0.888	2.608	138.09	3.322	Cl7	[-x+1/2, -y+3/2, z+1/2]
N2-H2B	0.888	2.9	114.3	3.364	Cl6	
N2-H2C	0.89	2.42	166.91	3.293	Cl15	[-x+1, -y+2, z]

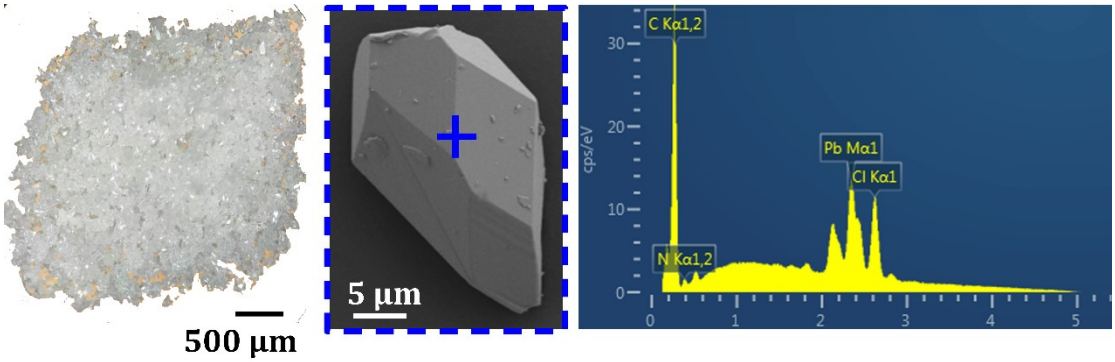

	Pb	Cl	C	N
Experimental (%)	54.3	26.61	7.92	4.47
Theoretical (%)	58.7	28.12	8.16	3.17

Figure S1. The Bulk single crystals of $(H_2MPP)_2Pb_5Cl_{14}$, SEM image of a selected microcrystal of $(H_2MPP)_2Pb_5Cl_{14}$, and the elemental analysis result for Pb, Cl, C, and N in $(H_2MPP)_2Pb_5Cl_{14}$.

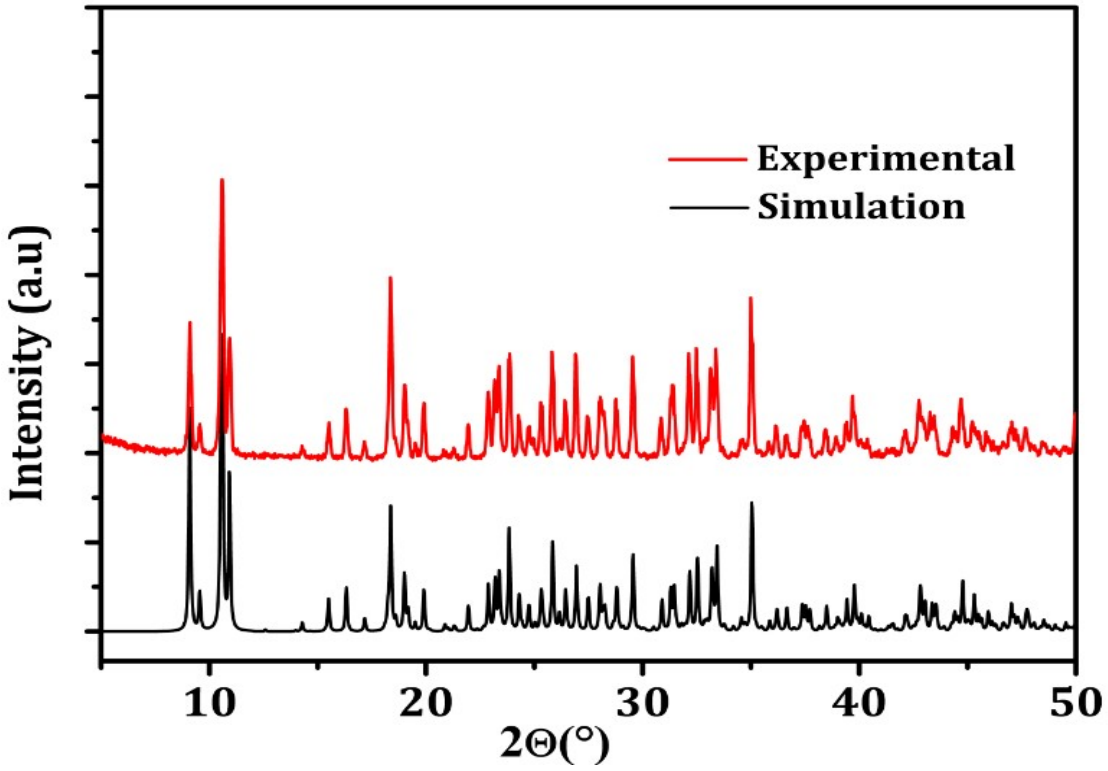

Figure S2. The experimental PXRD pattern of $(H_2MPP)_2Pb_5Cl_{14}$ in comparison to its simulation pattern.

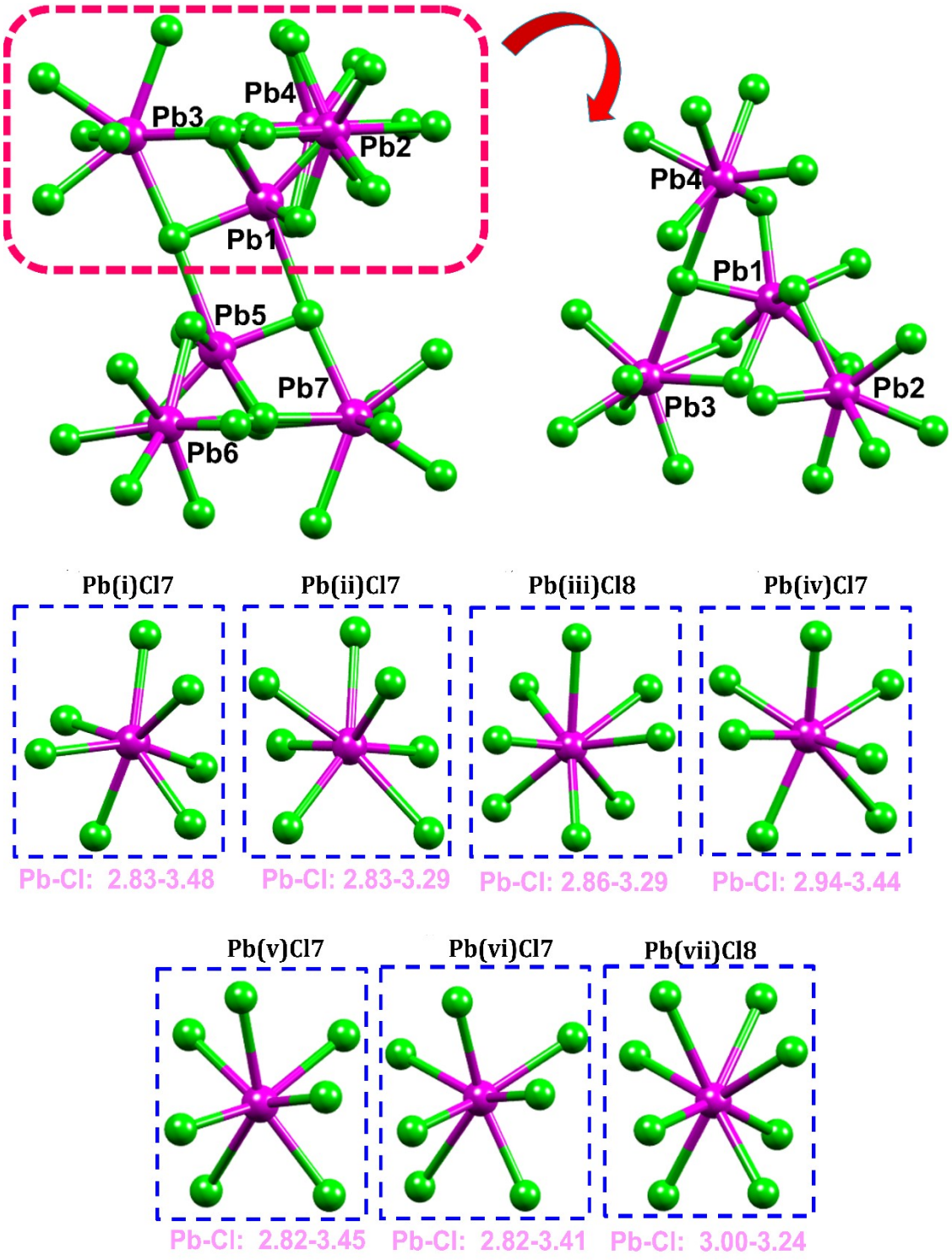

Figure S3. The coordinate environment and Pb-Cl bond lengths of seven individual polyhedral, [Pb(i)Cl_7], [Pb(ii)Cl_7], [Pb(iii)Cl_8], [Pb(iv)Cl_7], [Pb(v)Cl_7], [Pb(vi)Cl_7], [Pb(vii)Cl_8], in $(H_2MPP)_2Pb_5Cl_{14}$ crystal structure.

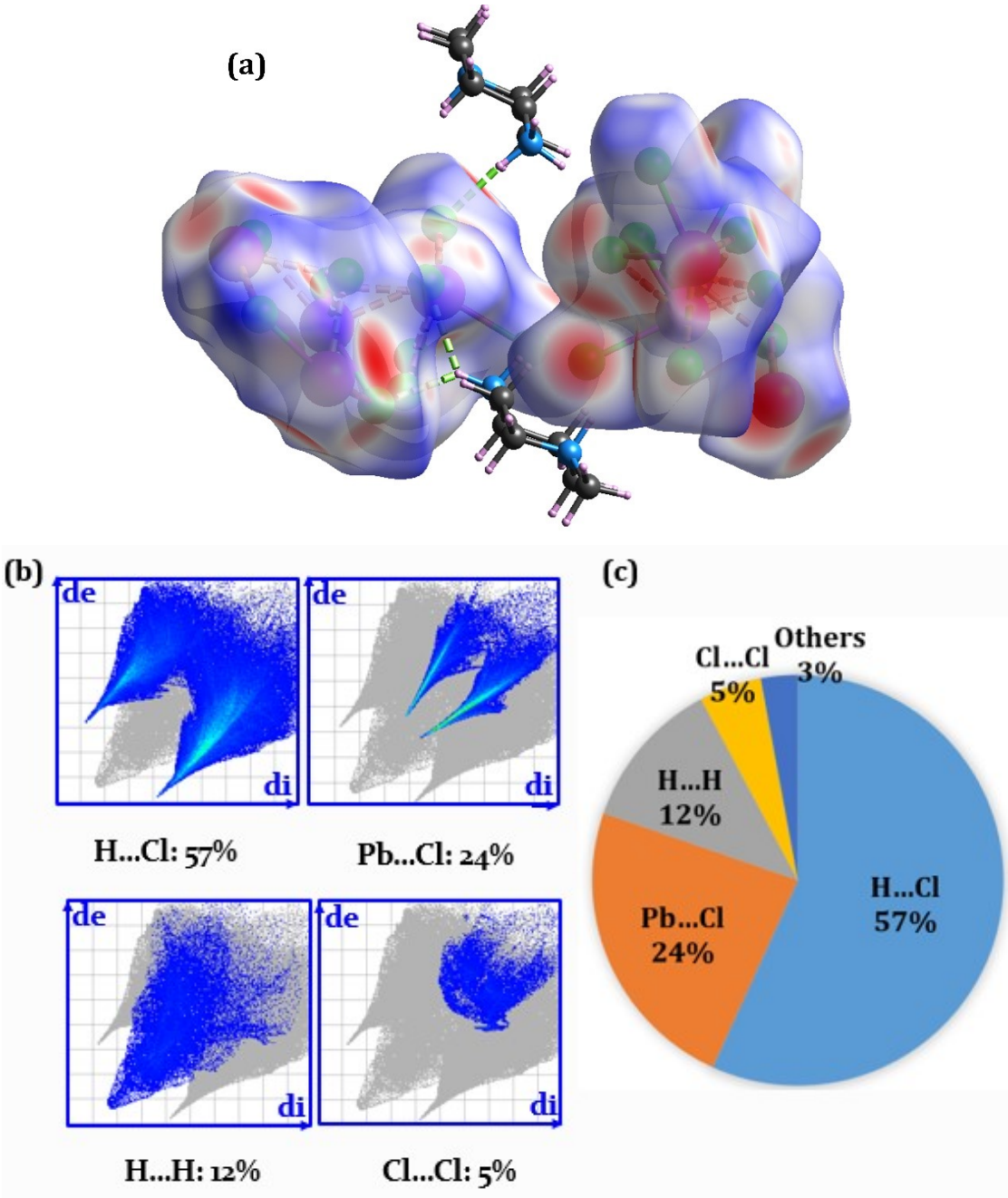

Figure S4. (a) Hirshfeld surfaces mapped with dnorm for $(H_2MPP)_2Pb_5Cl_{14}$ (color coding: white, distance d equals VDW distance; blue, d exceeds VDW distance, red, d, smaller than VDW distance). (b) Two-dimensional finger prints plots for $(H_2MPP)_2Pb_5Cl_{14}$. (c) The population of close contacts for $(H_2MPP)_2Pb_5Cl_{14}$ in crystal stacking.

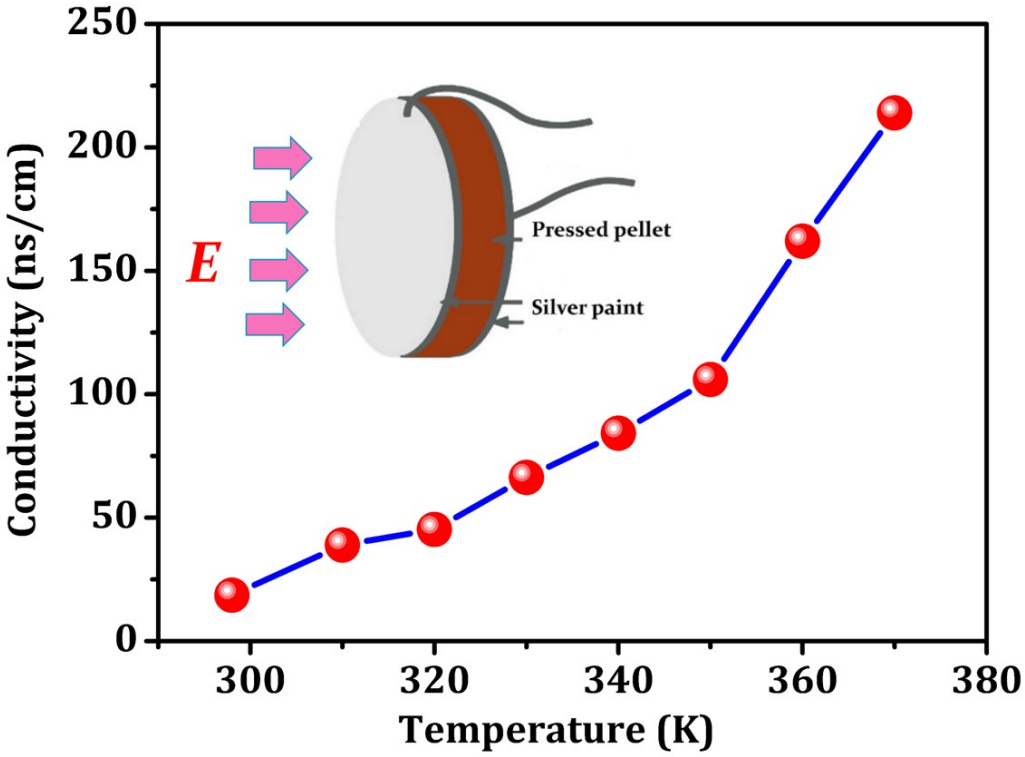

Figure S5. electrical conductivity of $(H_2MPP)_2Pb_5Cl_{14}$ at different temperatures.

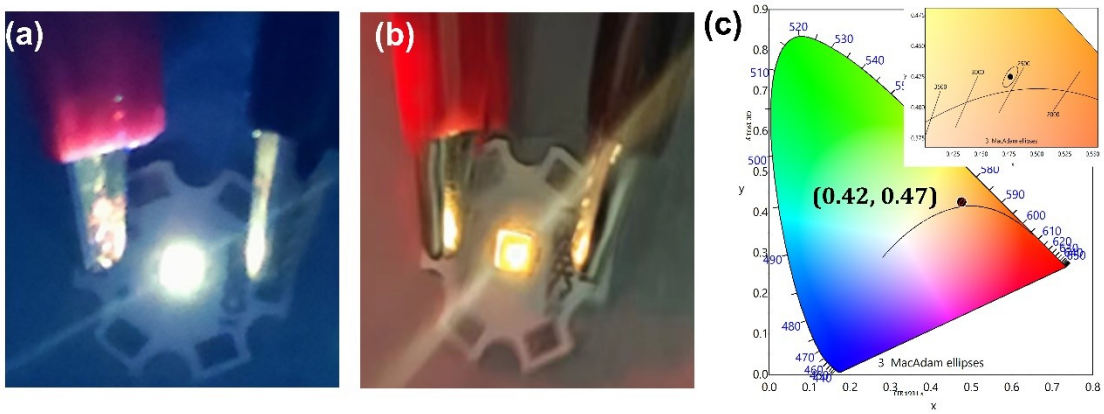

Figure S6. Photograph of UV-pumped LED with an excitation wavelength of 290 nm before (a) and after (b) pasting $(H_2MPP)_2Pb_5Cl_{14}$. (c) corresponding CIE 1931 chromaticity coordinate of $(H_2MPP)_2Pb_5Cl_{14}$.

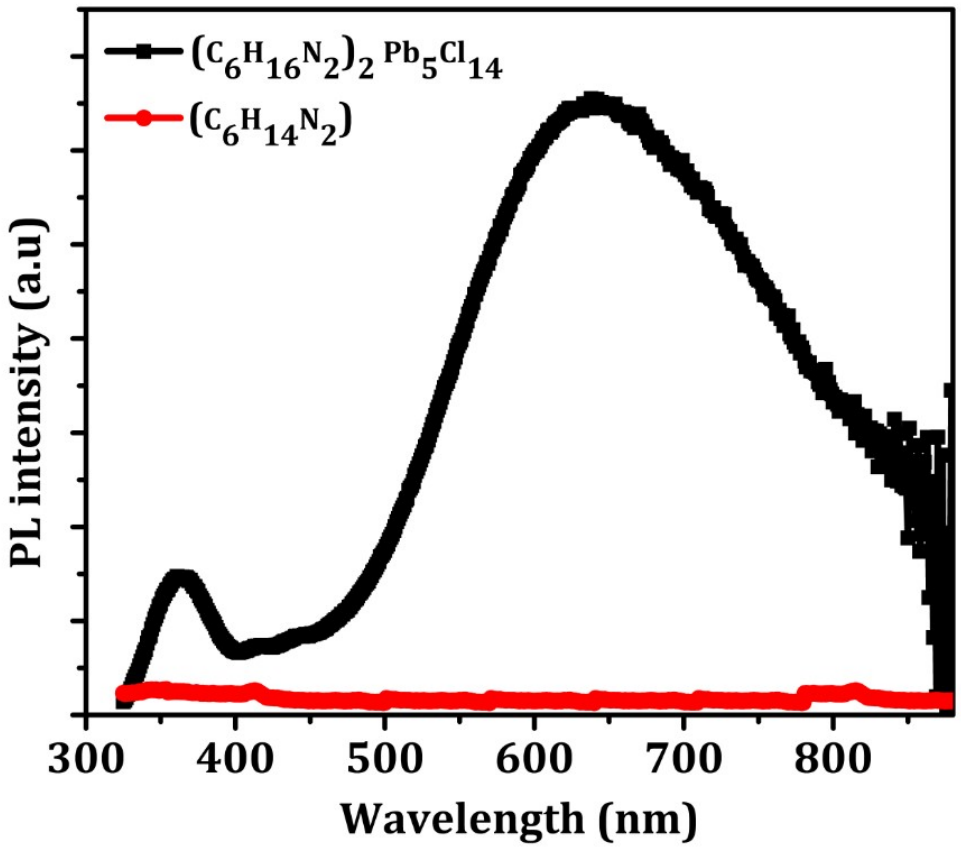

Figure S7. Comparison of PL intensity between $C_6N_2H_{14}$ and $(C_6N_2H_{16})_2Pb_5Cl_{14}$

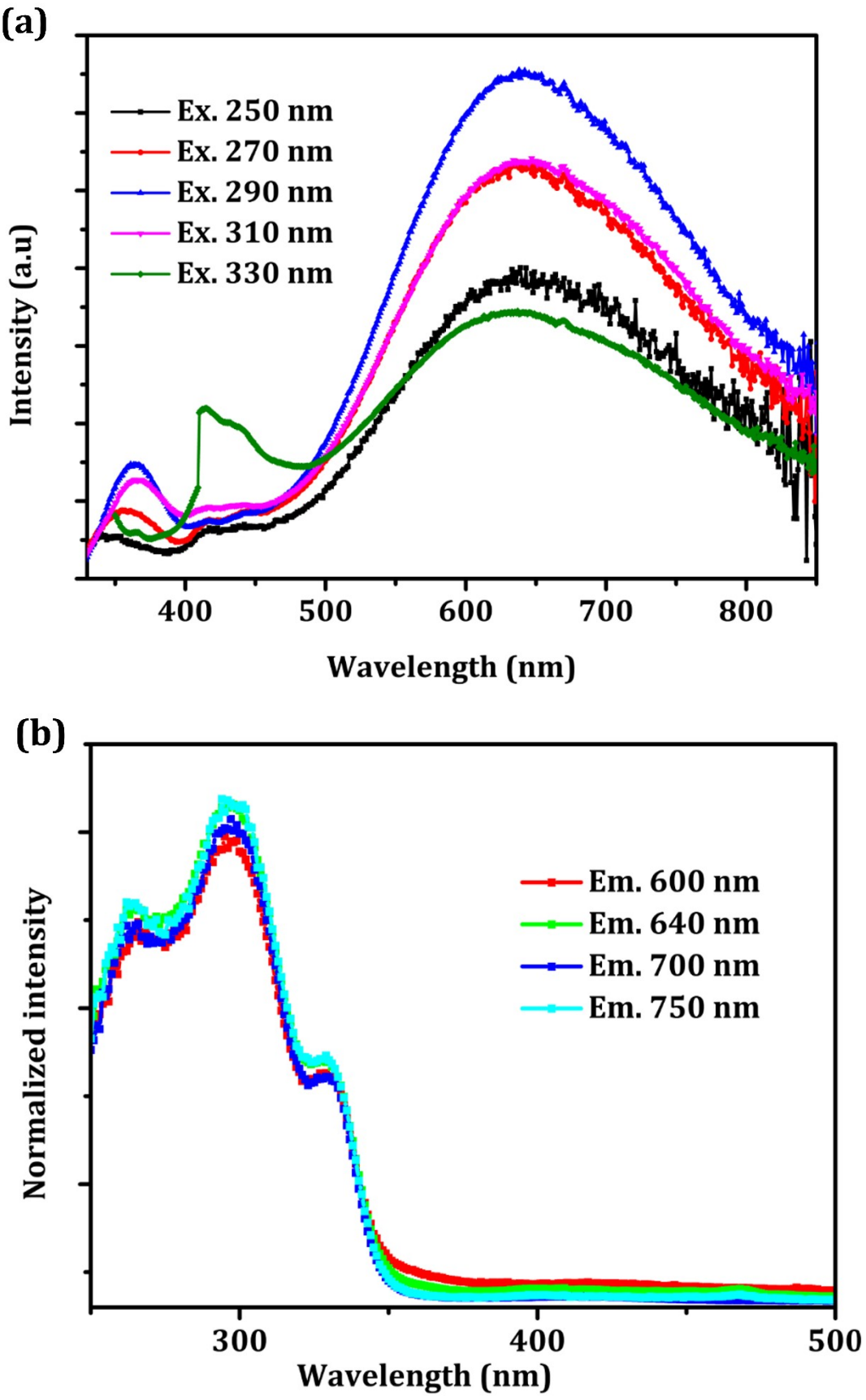

Figure S8. (a) The normalized excitation-dependent PL spectra. (b) The normalized emission-dependent PLE spectra of $(H_2MPP)_2Pb_5Cl_{14}$.

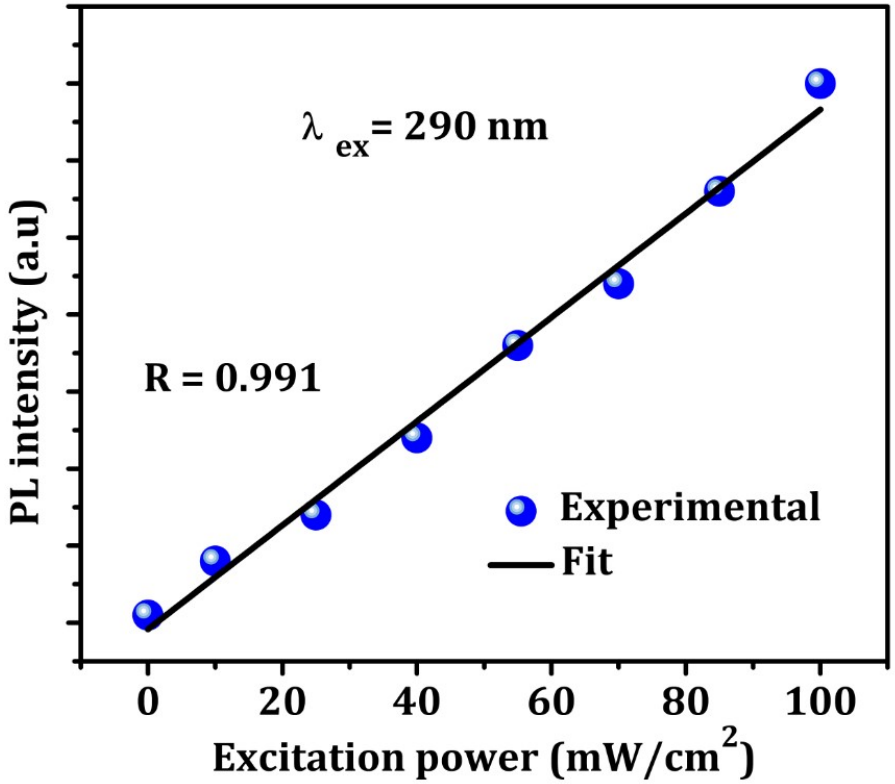

Figure S9. The PL intensity versus excitation power of $(H_2MPP)_2Pb_5Cl_{14}$ measured at room temperature.

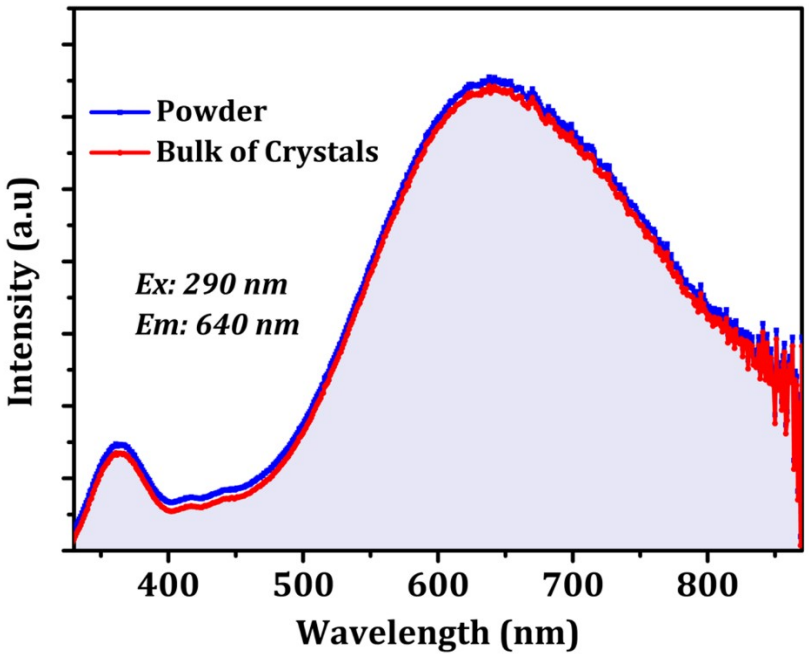

Figure S10. PL spectra of the bulk single crystal and milled-powders of $(H_2MPP)_2Pb_5Cl_{14}$ under 290 nm excitation

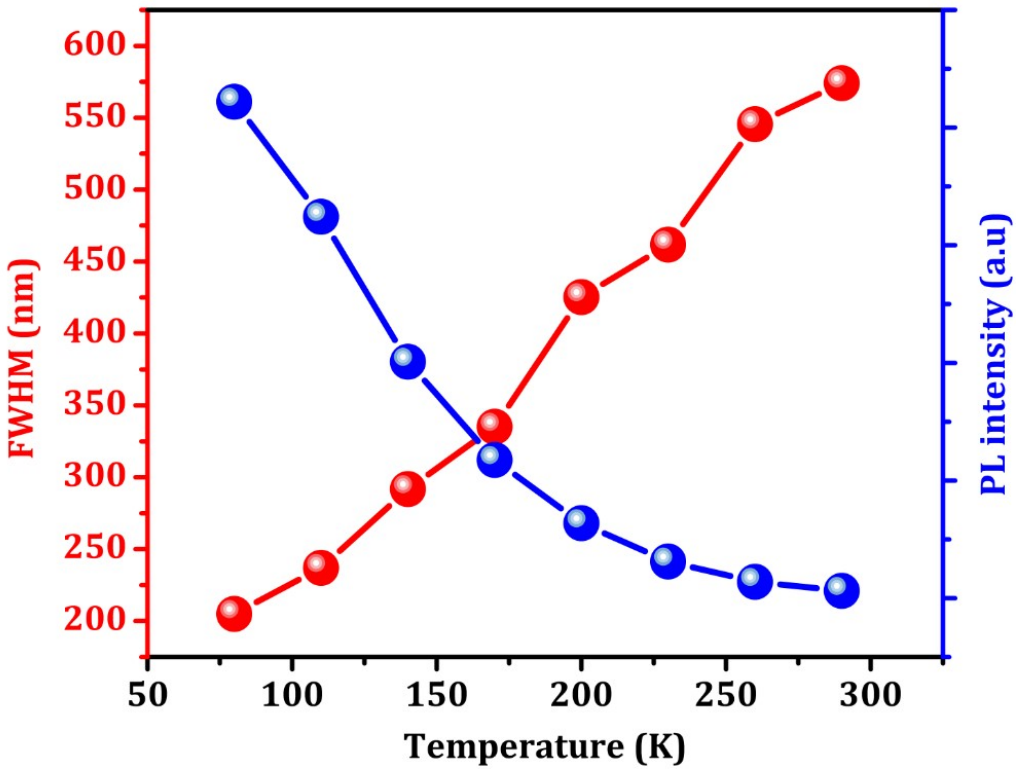

Figure S11. Plot of the maximum PL intensity (bleu) and FWHM (red) vs temperature (T).

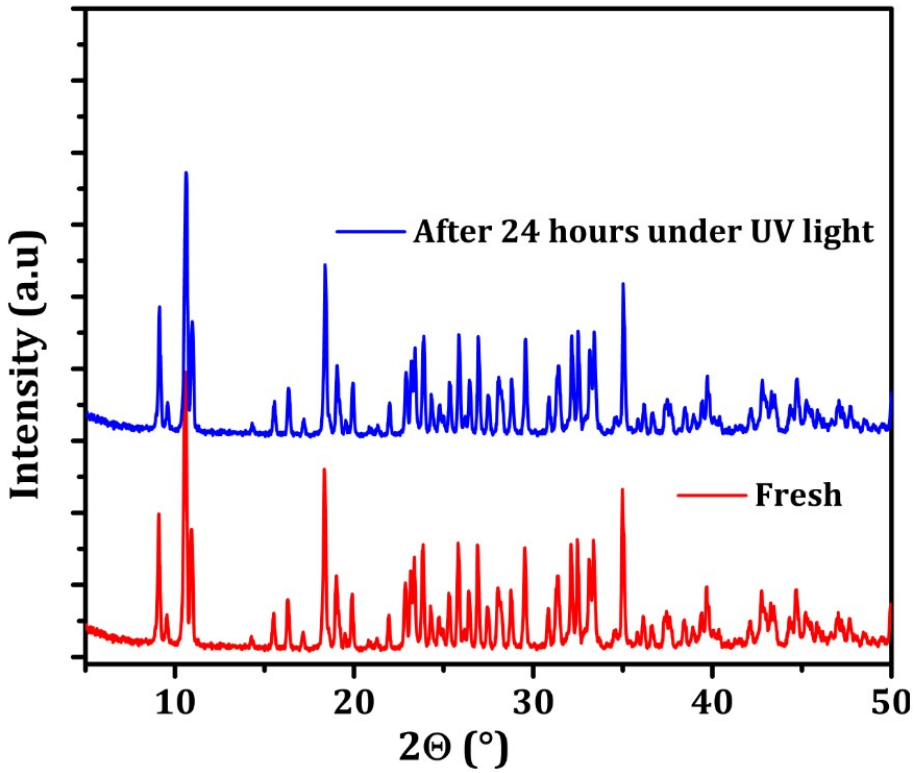

Figure S12. The PXRD patterns of $(H_2MPP)_2Pb_5Cl_{14}$ at the initial and after exposure to UV light for 24 hours.

References

[S1] Sheldrick G. A Short History of Shelx [J]. Acta Crystallographica Section A. 2008, 64(1), 112-122.

[S2] F. E. M. O'BRIEN, The Control of Humidity by Saturated Salt Solutions, J. Sci. Instrum. 1948, 25, 73–76.

[S3] J. Hafner, J. Comput. Chem. 2008. 29, 2044-2078.

[S4] Perdew J P, Burke K, Ernzerhof M. Generalized Gradient Approximation Made Simple [J]. Physical Review Letter. 1996, 77(18), 3865-3868.

[S5] D. M. Ceperley and B. J. Alder, Ground-state of the electron-gas by a stochastic method. Phys. Rev. Lett. 1980, 45, 566.

[S6] J. P. Perdew and A. Zunger, Phys. Rev. B: Condens. Matter Mater. Phys. 1981, 23, 5048